



Photodegradation of para-nitrophenol catalyzed by Fe₂O₃/FeS nanocomposite

H.R. Pouretedal^{a,*}, M. Tavakkoli^b

^aFaculty of Applied Chemistry, Malek-ashtar University of Technology, Shahin-Shahr, Iran
Tel. +98 312 5912253; Fax: +98 312 5220420; email: HR_POURETEDAL@mut-es.ac.ir

^bDepartment of Chemistry, Islamic Azad University, Shahreza Branch, Shahreza, Iran

Received 24 September 2012; Accepted 24 November 2012

ABSTRACT

The Fe₂O₃/FeS nanocomposite is prepared in a colloidal solution and precipitation method. Characterization of Fe₂O₃/FeS nanocomposite is studied by X-ray diffraction, diffuse reflectance spectroscopy, energy dispersive X-ray spectroscopy, and transmission electron microscopy. The transmission electron microscope image shows the particles size less than 15 nm for nanocomposite. The band-gap energy of prepared nanocomposite is obtained 2.0 eV and thus the nanocomposite is active in visible region of radiation. The pollutant of para-nitrophenol (PNP) is degraded more than 98% at presence of Fe₂O₃/FeS nanocomposite (1.0 g/L) at time 180 min. The photocatalytic activity of nanocomposite is compared to Fe₂O₃ and FeS nanoparticles. The pseudo-first-order rate constant of photodegradation reaction of PNP (10 mg/L) is obtained 20.0×10^{-3} , 16.0×10^{-3} , and $6.5 \times 10^{-3} \text{ min}^{-1}$ at presence Fe₂O₃/FeS, FeS, and Fe₂O₃, respectively. The less band-gap energy vs. Fe₂O₃ and more reusability vs. FeS are the advantages of proposed photocatalyst.

Keywords: Nanocomposite; Para-nitrophenol; Photodegradation; Photocatalyst

1. Introduction

Environmental pollution is a greatest problem that caused a large number of researches of chemical scientists in background of photocatalyst and photodegradation process is focused for the solution [1]. The photocatalytic process is valuable when the proposed new photocatalysts show a photocatalytic activity in solar spectrum and not merely the scarcely available UV spectrum. The preparation of photocatalysts active in visible spectrum and stable against the photocorrosion is a relatively recent objective that has been intensively researched only during the past

decade. Stability is a critical factor in photocatalytic reactions [2–4].

Metal sulfide semiconductors, such as CdS and FeS, have a desirably small band gap that is an advantage but photoanodic corrosion of their due to the energetically unfavorable position of valance band edge is a limitation [5]. These semiconductors indicate the extremely short photocatalytic lifetime, where the exact time depends on the reaction environment. Other catalysts such as metal oxides are suitable photocatalysts for various UV applications, although this semiconductor undergoes photocathodic corrosion when in aqueous solutions, eliminating it as a potential catalyst for many applications [6]. The ideal

*Corresponding author.

photocatalyst should be photochemically stable and therefore insusceptible to any type of corrosion in all reaction environments [7,8].

Although many questions still exist in about the interaction mechanisms between the particles in a composite, but researches on the coupling of semiconductor photocatalysts as nanocomposite alloys has taken place in last decade [9–12]. There is little doubt that the effectiveness of the coupling of nanoparticle semiconductor photocatalysts is due at least in part to interfacial charge transfer between two different semiconductors with disparately favorable band edge energy levels. The band gaps and energy band levels for most metal oxides and sulfides have been provided in literature [10,11]. The coupled semiconductors have photocatalytic activity under visible light irradiation, however, they are plagued with unfavorable characteristics such as toxicity and susceptibility to photoanodic corrosion [10,11].

Iron oxide (α -Fe₂O₃) has been attracting attention as a potential photocatalyst because it is stable, safe, and inexpensive among the conventional photocatalysts working under visible-light irradiation [13,14]. The photocatalytic activity of α -Fe₂O₃ was found to depend on its particle size. This is because its photo-generated carriers have a short diffusion length (\approx 20 nm). Therefore, the study of the fabrication of fine Fe₂O₃ particles has been conducted with an aim to establish an efficient photocatalysis system [15,16].

Iron sulfide minerals show unique magnetic and electrical properties, which are related to the stoichiometric ratio between Fe and S as well as their crystalline structure [17,18]. Recent studies have reported the synthesis of sheet-like FeS that exhibits peroxidase-like behavior and hydrogen peroxide sensing activity. Further, FeS possesses specific electron-transfer ability and good adsorption characteristic, and more importantly, has a lower band gap than FeO [19].

In this paper, we reported the synthesis and characterization of Fe₂O₃/FeS nanocomposite. We demonstrate that Fe₂O₃/FeS nanocomposites show the higher photocatalytic activity in degradation of p-nitrophenol (PNP) vs. Fe₂O₃ and FeS nanoparticles alone.

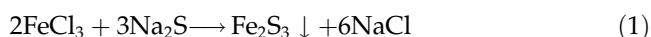
2. Experimental

2.1. Synthesis of photocatalysts

Fe₂O₃ nanoparticles powder was prepared by precipitation method. FeCl₃·6H₂O was used as the starting materials, and ammonia (1:1) was used as the precipitator. The Fe³⁺ solution (250 ml of 0.02 mol/L) was stirred at room temperature and added drop-wise with the ammonia until it transformed to precipitate

completely (pH 3.5). The precipitate was filtered and washed with deionized water until no Cl⁻ was found in the filtrates. Then the wet powder was dried at about 100°C in air to form the precursor of the Fe₂O₃ photocatalyst. Finally, the precursor was calcined for 3 h at various temperatures (200–600°C) in air to prepare the photocatalyst powder.

The precipitation method with Na₂S·9H₂O as precipitant agent and FeCl₃·6H₂O as precursor was used to prepared FeS nanoparticles. About 75 ml S²⁻ solution was added drop-wise to 250 ml of 0.02 mol/L Fe³⁺ solution. Fe₂S₃ is prepared by addition of refrigerated iron(III) chloride dilution to also cooled sodium sulfide dilution.



which decays at a temperature over 20°C into FeS and sulfur.



The FeS nanoparticles was heated at 100°C and calcined for 3 h at temperatures of 200–600°C.

In order to preparation of Fe₂O₃/FeS nanocomposite, 25 ml S²⁻ solution was added drop-wise to 250 ml of 0.02 mol/L Fe³⁺ solution and then the pH of resulted solution is controlled at pH of 3.5 with addition of ammonia (1:1) solution. The obtained precipitate was filtered, washed, and heated at 100°C. Finally, the resulted composite was calcined for 3 h at temperatures of 200–600°C.

2.2. Characterization of nanocomposite

A Diffractometer Bruker D8ADVANCE Germany with anode of Cu ($\lambda = 1.5406 \text{ \AA}$ of Cu—K_α) and filter of Ni applied to record of X-ray diffraction (XRD) pattern of nanocomposite. The nanocomposite particles size is estimated by a JEOL JEM-1200EXII transmission electron microscope (TEM) operating at 120 kV. The supporting grids were formvar-covered, carbon-coated, 200-mesh copper grids. The composition of Fe₂O₃/FeS nanocomposite is evaluated by energy dispersive X-ray spectrometer by using a Philips XL30 scanning electron microscope. Diffuse reflectance spectra of nanocomposite are recorded on a Shimadzu UV-265 instrument using optical grade BaSO₄ as the reference.

2.3. Photodegradation of PNP

The photodegradation of PNP is performed at presence of Fe₂O₃, FeS, and Fe₂O₃/FeS nanoparticles. A photocatalytic reactor with a 36 W mercury low

pressure lamp as irradiation source is used to perform of photodegradation reactions. The light path is 3.0 cm in photoreactor cell. The photoreactor filled with 25 ml of 10–50 mg/L of PNP and 0.1–1.2 g/L of photocatalysts at pH 3–12. The whole reactor cooled with a water-cooled jacket on its outside and the temperature was kept at 25°C. All reactants in a degradation reaction stirred using a magnetic stirrer to uniform of photoreactor cell in duration time 30–180 min. In order to setting the adsorption/desorption equilibrium of PNP on heterogeneous catalysts surface, the reactor is kept in dark for 30 min.

The degradation efficiency of PNP determined with measurement of absorbance of samples by a UV-Vis spectrophotometer Carry-100 using a paired 1.0 cm quartz cell. The samples centrifuged to remove the heterogeneous photocatalysts before absorbance measurement. The absorbance of samples before (A_0) and after a distinct time (A_t) of irradiation and Beers' law to determination of C_0 and C_t is used to calculate the degradation efficiency ($\%D = 100 \times [1 - (C_t/C_0)] = 100 \times [1 - (A_t/A_0)]$).

3. Results and discussion

3.1. Characterization of Fe_2O_3/FeS nanocomposite

An XRD study shows that synthesized Fe_2O_3/FeS nanocomposites have a cubic structure which is similar to PDF No- 01-089-5892 for γ - Fe_2O_3 [15,16]. The Scherrer formula show the average crystal size of 13 nm for nanocomposite by using peak of (311) (Fig. 1).

Reflectance spectroscopy is the study of light as a function of wavelength that has been reflected or scattered from a solid, liquid, or gas. Fig. 2 shows the diffuse reflectance spectra of Fe_2O_3 , FeS, and Fe_2O_3/FeS nanocomposites. It is revealed that the wavelength of excitation of Fe_2O_3 , FeS, and Fe_2O_3/FeS nanoparticles are 538, 615, and 620 nm, respectively, that is equivalent 2.5, 2.1, and 2.0 eV of band-gap energy of photocatalysts. The reported band-gap energies of Fe_2O_3 and FeS particles are 2.2 and 1.8 eV, respectively [6,7,19]. Thus, a reduction in band-gap is seen for Fe_2O_3 and FeS nanoparticles in comparison to their particles. The band-gap energy of Fe_2O_3/FeS

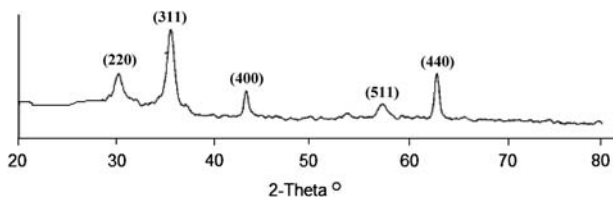


Fig. 1. The XRD pattern of Fe_2O_3/FeS nanocomposite calcined at 300°C.

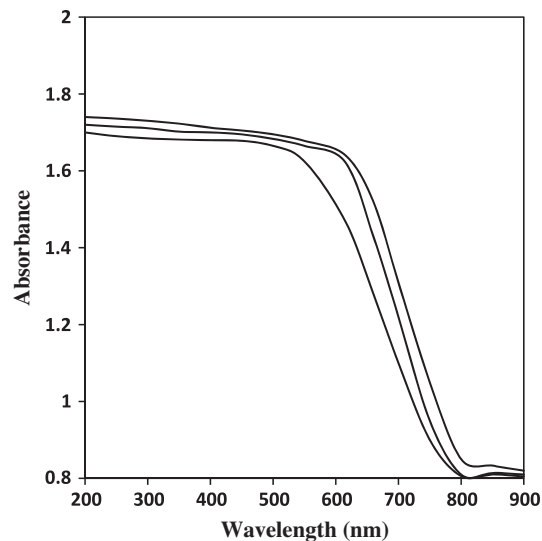


Fig. 2. The diffuse reflectance spectra of Fe_2O_3 , FeS, and Fe_2O_3/FeS nanocomposite calcined at 300°C (from down to up).

nanocomposite is lowest and it is expected the higher production of electron-hole under similar irradiation.

The simultaneous Energy dispersive X-ray (EDX) analysis indicates the presence of Fe, S, and O in the prepared nanocomposite (Fig. 3). EDX spectra collected from five differently elected regions gave similar results. The weight percent of O and S is obtained 17.8 and 11.5%, respectively, that show approximately atomic ratio of 3:1 for oxygen:sulfur in prepared nanocomposites. Thus, the formation of Fe_2O_3/FeS nanocomposite is also confirmed by using EDX analysis.

The TEM images of Fe_2O_3/FeS nanocomposite treated at 300°C are shown in Fig. 4. It is seen that the prepared nanocomposites are agglomerated with an average size of less than 15 nm. The TEM analysis also shows the nanoparticles have a slightly irregular and rounded shape.

3.2. PNP photodegradation

One the very important parameters that influence the photocatalytic activity of photocatalysts and photodegradation efficiency are pH of samples. The charge of pollutant molecules and surface charge of heterogeneous catalysts are dependent pH variable. The effect of pH samples on the photodegradation efficiency is indicated in Fig. 5. The conditions are 0.1 g/L photocatalyst, PNP 10 mg/L, calcinations temperature 300°C, and irradiation time 180 min. As seen, the highest photodegradation yield is obtained at pH 10. Point of zero charge of Fe_2O_3 and FeS is reported at pH 6.2–6.8 and 3.3, respectively [20,21]. Therefore, the surface charge of photocatalysts is negative in $pH > 7$. The

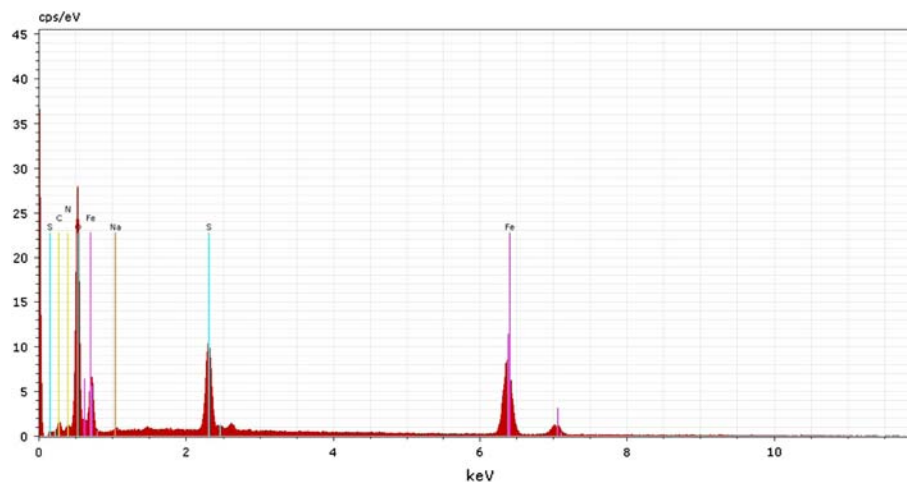


Fig. 3. The EDX spectra of $\text{Fe}_2\text{O}_3/\text{FeS}$ nanocomposite calcined at 300°C .

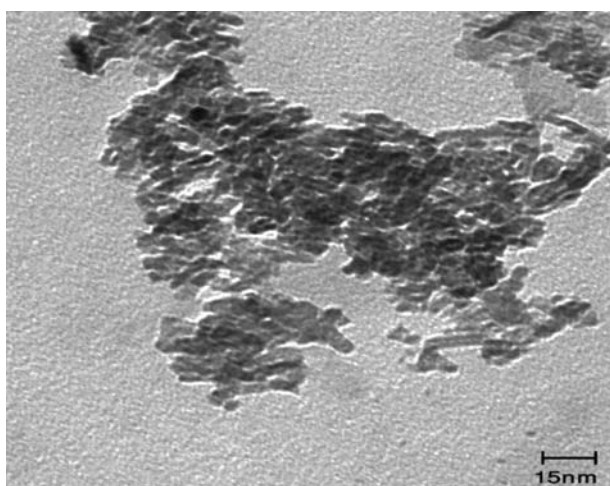


Fig. 4. The TEM image of $\text{Fe}_2\text{O}_3/\text{FeS}$ nanocomposite calcined at 300°C .

hydroxide ion concentration is increased in alkaline pHs and thus, the hydroxyl radical as an active reagent increase with enhancement of pH. But, in $\text{pH} > 10$, the ionization of PNP molecules is due to formation of anions of PNP. The repulsive of negative ions of pollutant molecules and also hydroxide ions with photocatalyst particles with negative surface charge is due to a decrease in surface probability adsorption of them [22]. Therefore, a reduction in degradation efficiency is observed at $\text{pH} > 10$.

The particles size of photocatalysts can be related to calcinations temperature. The effect of calcinations temperature ($200\text{--}600^\circ\text{C}$) on the degradation efficiency is shown in Fig. 6. Apparently, the agglomeration of nanoparticles is occurred with an increase in calcinations of temperature. The decrease of catalyst surface and the number of adsorbed pollutant mole-

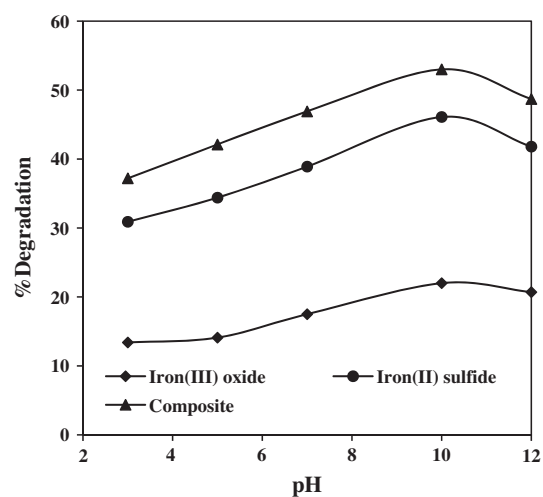


Fig. 5. The effect of pH on the photodegradation efficiency of PNP (10 mg/L), 0.1 g/L of photocatalyst, irradiation time 180 min .

cules are observed upon this agglomeration [23,24]. As well as particles size, the dose of photocatalysts also influence on the catalyst surface and degradation efficiency. The effect of catalyst dose is indicated in Fig. 7. The photodegradation efficiency of PNP is increased with increasing the amount of photocatalyst from 0.1 to 1.0 g/L and then diminishes with loading of photocatalyst above of 1.0 g/L . As the loading is increased beyond the optimum amount, due to an increase in turbidity of the suspension, a decreasing is seen in penetration of light and photoactivated volume of suspension. In these conditions, the penetration depth of the photons is decreased and less catalyst nanoparticles could be activated [25,26].

The kinetic rate constants of PNP ($10\text{--}50\text{ mg/L}$) photodegradation are brought in Table 1. The pseudo-

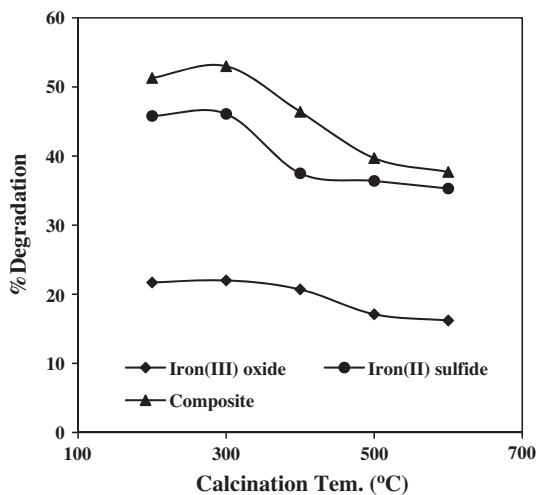


Fig. 6. The effect of calcinations temperature of prepared photocatalysts on the photodegradation efficiency of PNP (10 mg/L), 0.1 g/L of photocatalyst, pH 10, and irradiation time 180 min.

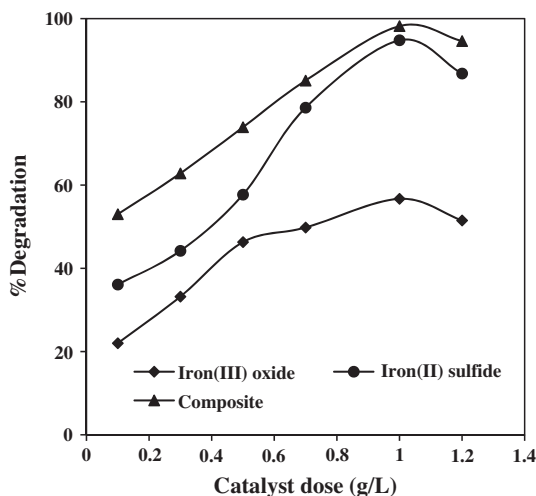


Fig. 7. The effect of dosage of catalyst on the photodegradation efficiency of PNP (10 mg/L), pH 10, and irradiation time 180 min.

first-order rate constants, k_{obs} (min^{-1}), are obtained using Langmuir–Hinshelwood kinetic expression ($\ln(C_o/C_t) = k_{obs}t$) [27].

As seen from Table 1 data, the pseudo-first-order rate constants decrease with increasing of initial concentration of PNP. The high adsorption of PNP molecules on the substrate, decreasing generation of hydroxyl radicals in active sites and increasing absorption of photons by PNP molecules are due to reduction of degradation efficiency at high concentrations of pollutant [28,29].

As seen from the Figs. 5–7 and data of Table 1, the photocatalytic activity of prepared photocatalysts is $\text{Fe}_2\text{O}_3/\text{FeS}$ nanocomposite > FeS nanoparticles > Fe_2O_3 nanoparticles. The band-gap energy of FeS (2.1 eV) is less than Fe_2O_3 (2.5 eV) nanoparticles and therefore increasing of hole-electron production yield in FeS semiconductor is respected under similar conditions. In natural, the more number of hole-electron is due to increasing of active radicals in photodegradation process. The band-gap energy of $\text{Fe}_2\text{O}_3/\text{FeS}$ nanocomposite is obtained 2.0 eV that near to E_g of FeS nanoparticles. The partial reduction of band-gap energy of $\text{Fe}_2\text{O}_3/\text{FeS}$ nanocomposite is due to partial increasing of photocatalytic activity. But, an important advantage of $\text{Fe}_2\text{O}_3/\text{FeS}$ nanocomposite vs. FeS nanoparticles is the more stability nanocomposite in photocorrosion process of photocatalyst.

The lower edge of the conduction band and the upper edge of the valence band of Fe_2O_3 is +0.4 and +2.5 V vs. normal hydrogen electrode. While, the $\text{Fe}^{3+}/\text{Fe}^{2+}$ redox couple show a potential of +0.77 V [30]. Apparently, the existence of $\text{Fe}^{3+}/\text{Fe}^{2+}$ in $\text{Fe}_2\text{O}_3/\text{FeS}$ nanocomposite and location of energy level of $\text{Fe}^{3+}/\text{Fe}^{2+}$ redox couple in band-gap of Fe_2O_3 can aid to electron transfer in semiconductor. The increasing of probability of electron transfer is due to increasing of electron-hole production.

So the photoactivity reproducibility of $\text{Fe}_2\text{O}_3/\text{FeS}$ nanocomposite is studied in a four cycle photodegradation. Each experiment is carried out with 10.0 mg/L of PNP, 1.0 g/L of nanocomposite, pH of

Table 1

The pseudo-first-order rate constants, k_{obs} (min^{-1}), of PNP photodegradation reaction catalyzed by prepared photocatalysts

Photocatalyst	Concentration of PNP (mg/L)				
	10	20	30	40	50
Fe_2O_3	6.5×10^{-3}	4.8×10^{-3}	4.0×10^{-3}	2.9×10^{-3}	2.3×10^{-3}
FeS	16.0×10^{-3}	8.0×10^{-3}	7.5×10^{-3}	5.0×10^{-3}	3.8×10^{-3}
$\text{Fe}_2\text{O}_3/\text{FeS}$	20.0×10^{-3}	9.3×10^{-3}	8.7×10^{-3}	5.7×10^{-3}	4.2×10^{-3}

10, at time of 180 min. After each experiment, the catalyst particles was removed, washed with water and ethanol solvent, and dried at 70–80°C temperature, and then used in a new experiment. The degradation for four cycles is 97–89% showing the best reproducibility and stability against of photocorrosion. While, the FeS nanoparticles indicated a two recyclability in PNP photodefraration reaction (%D = 93–79%).

4. Conclusion

The Fe₂O₃/FeS nanocomposite as a new photocatalyst shows a superior versus Fe₂O₃ and FeS nanoparticles. The proposed photocatalyst shows a less band-gap energy and more stability vs. Fe₂O₃ and FeS, respectively. The serious pollutant of para-nitrophenol can be efficiently degraded (>98%) at pH 10 and irradiation time 180 min at presence of 1.0 g/L of Fe₂O₃/FeS nanocomposite.

References

- [1] D.M. Blake, Bibliography of Work on the Photocatalytic Removal of Hazardous Compounds from Water and Air. Update Number 3, to January 1999. NREL/TP-570-26797. Golden, CO: National Renewable Energy Laboratory. pp. 163. Available from the National Technical Information Service, Springfield, VA 22161.
- [2] M. Hoffman, S. Martin, W. Choi, D. Bahnemann, Environmental applications of semiconductor photocatalysis, *Chem. Rev.* 95 (1995) 69–96.
- [3] A. Linsebigler, G. Lu, J. Yates, Photocatalysis on TiO₂ surfaces: Principle, mechanisms, and selected results, *Chem. Rev.* 95 (1995) 735–758.
- [4] Y. Goswami, Engineering of solar photocatalytic detoxification and disinfection processes, *Advances in Solar Energy* 10 (1995) 165–210.
- [5] W. Chengyu, S. Huamei, T. Ying, T. Tongsuo, Z. Guowu, Properties and morphology of CdS comounded TiO₂ visible-light activated photocatalytic nanofilms coated on glass surface, *Sep. Purif. Technol.* 32 (2003) 357–362.
- [6] M. Valenzuela, P. Bosch, J. Jimenez-Becerrill, O. Quiroz, A. Paez, Preparation, characterization and photocatalytic activity of ZnO, Fe₂O₃ and ZnFe₂O₄, *J. Photochem. Photobiol. A* 148 (2002) 177–182.
- [7] A. Mills, S. Le Hunte, An overview of semiconductor photocatalysis, *J. Photochem. Photobiol. A* 108 (1997) 1–35.
- [8] I. Shkrob, M. Sauer, Hole scavenging and photo-stimulated recombination of electron-hole pairs in aqueous TiO₂ nanoparticles, *J. Phys. Chem. B* 4 (2004) 1–63.
- [9] A. Nezamzadeh-Ejhi, Z. Banan, Sunlight assisted photodecolorization of crystal violet catalyzed by CdS nanoparticles embedded on zeolite A, *Desalination* 284 (2012) 157–166.
- [10] V. Sharma, N. Gandhi, A. Khant, R.C. Khandelwal, E. Nhandced, Photodegradation of azure B by coprecipitated NiS-ZnS (1: 5), *Int. J. Chem. Sci.* 8 (2010) 1965–1972.
- [11] H. Kim, J. Kim, W. Kim, W. Choi, Enhanced photocatalytic and photoelectrochemical activity in the ternary hybrid of CdS/TiO₂/WO₃ through the cascaded electron transfer, *J. Phys. Chem. C* 115 (2011) 9797–9805.
- [12] C. Shifu, L. Wei, Z. Sujuan, C. Yinghao, Preparation and activity evaluation of relative p–n junction photocatalyst Co-TiO₂/TiO₂, *J. Sol-Gel Sci. Technol.* 54 (2010) 258–267.
- [13] S. Kakuta, T. Abe, Photocatalysis for water oxidation by Fe₂O₃ nanoparticles embedded in clay, *J. Mater. Sci.* 44 (2009) 2890–2898.
- [14] A. Duret, M. Gratzel, Visible light-induced water oxidation on mesoscopic α -Fe₂O₃ films made by ultrasonic spray pyrolysis, *J. Phys. Chem. B* 109 (2005) 17184–17191.
- [15] H. Xia, H. Zhuang, T. Zhang, D. Xiao, Visible-light-activated nanocomposite photocatalyst of Fe₂O₃/SnO₂, *Mater. Lett.* 62 (2008) 1126–1128.
- [16] C. Karunakaran, S. Senthilvelan, Fe₂O₃-photocatalysis with sunlight and UV light: Oxidation of aniline, *Electrochem. Commun.* 8 (2006) 95–101.
- [17] C.N.R. Rao, K.P.R. Pisharody, Formation of iron sulfide nodules during anaerobic oxidation of methane, *Prog. Solid State Chem.* 10 (1976) 207–270.
- [18] D. Rickard, G.W. Luther, Chemistry of iron sulfides, *Chem. Rev.* 107 (2007) 514–562.
- [19] S.K. Maji, A.K. Dutta, P. Biswas, D.N. Srivastava, P. Paul, A. Mondal, B. Adhikary, Synthesis and characterization of FeS nanoparticles obtained from a dithiocarboxylate precursor complex and their photocatalytic, electrocatalytic and biomimic peroxidase behavior, *Appl. Catal. A* 419–420 (2012) 170–177.
- [20] S. Mustafa, S. Tasleem, A. Naeem, Surface charge properties of Fe₂O₃ in aqueous and alcoholic mixed solvents, *J. Colloid Interface Sci.* 275 (2004) 523–529.
- [21] S. Chibowski, W. Janusz, Specific adsorption of Zn(II) and Cd(II) ions at the α -Fe₂O₃/electrolyte interface structure of electrical double layer, *Appl. Surface Sci.* 196 (2002) 343–355.
- [22] H.R. Pouretedal, Z. Tofangsazi, M.H. Keshavarz, Photocatalytic activity of mixture of ZrO₂/SnO₂, ZrO₂/CeO₂ and SnO₂/CeO₂ nanoparticles, *J. Alloys Comp.* 513 (2012) 359–364.
- [23] H.R. Pouretedal, M. Hosseini, Bleaching kinetic and mechanism study of congo red catalyzed by ZrO₂ nanoparticles prepared by using a simple precipitation method, *Acta Chim. Slov.* 57 (2010) 415–423.
- [24] H.R. Pouretedal, A. Kadkhodaie, Synthetic CeO₂ nanoparticle catalysis of methylene blue photodegradation: Kinetics and mechanism, *Chin. J. Catal.* 31 (2010) 1328–1334.
- [25] S. Ahmed, M.G. Rasul, W.N. Martens, R. Brown, M.A. Hashib, Heterogeneous photocatalytic degradation of phenols in wastewater: A review on current status and developments, *Desalination* 261 (2010) 3–18.
- [26] Q. Zhuo, H. Ma, B. Wang, F. Fan, Degradation of methylene blue: Optimization of operating condition through a statistical technique and environmental estimate of the treated wastewater, *J. Hazard. Mater.* 153 (2008) 44–51.
- [27] G. Sivalingam, M.H. Priya, Giridhar Madras, Kinetics of the photodegradation of substituted phenols by solution combustion synthesized TiO₂, *Appl. Catal. B* 51 (2004) 67–76.
- [28] H.R. Pouretedal, M.H. Keshavarz, Synthesis and characterization of Zn_{1-x}Cu_xS and Zn_{1-x}Ni_xS nanoparticles and their applications as photocatalyst in Congo red degradation, *J. Alloys Comp.* 501 (2010) 130–135.
- [29] M. Grätzel, Photoelectrochemical cells, *Nature* 414 (2001) 338–344.
- [30] H.R. Pouretedal, S. Narimany, M.H. Keshavarz, Nanoparticles of ZnS doped with iron as photocatalyst under UV and sunlight irradiation, *Int. J. Mat. Res.* 101 (2010) 1046–1051.